

Low temperature crystallization of $\text{Cu}_2\text{ZnSnSe}_4$ thin films using binary selenide precursors

Rhishikesh Mahadev Patil¹ · Dipak Ramdas Nagpure¹ · G. Swapna Mary¹ · G. Hema Chandra¹ · M. Anantha Sunil² · Y. P. Venkata Subbaiah³ · P. Prathap⁴ · Mukul Gupta⁵ · R. Prasada Rao⁶

Received: 22 February 2017 / Accepted: 19 August 2017 / Published online: 31 August 2017
© Springer Science+Business Media, LLC 2017

Abstract In the present paper, a novel process for synthesis of $\text{Cu}_2\text{ZnSnSe}_4$ thin films via low temperature selenization (350 °C) of multiple stacks of binary selenides has been reported. Further, the influence of selenization temperature (250–450 °C) on the physical properties of $\text{Cu}_2\text{ZnSnSe}_4$ thin films was studied and discussed herein. The Rietveld refinement from X-ray diffraction data of $\text{Cu}_2\text{ZnSnSe}_4$ films grown at a selenization temperature of 350 °C was found to be single phase with kesterite type crystal structure and having lattice parameters $a = 5.695 \text{ \AA}$, $c = 11.334 \text{ \AA}$. Raman spectra recorded using multi excitation wavelength sources under non-resonant and near resonant conditions confirms the formation of single phase $\text{Cu}_2\text{ZnSnSe}_4$ films. Secondary ion mass spectroscopic (SIMS) analysis demonstrated that

composition of elements across the thickness is fairly uniform. Energy dispersive X-ray analysis measurement reveals that the obtained films are Cu-poor and Zn-rich. The scanning electron micrographs of binary selenide stacks selenized at a temperature of 350 °C shows randomly oriented cylindrical grains. The optical absorption studies indicated a direct band gap of 1.01 eV. The films showed *p*-type conductivity with electrical resistivity of 4.66 $\Omega \text{ cm}$, Hall mobility of 15.17 $\text{cm}^2 (\text{Vs})^{-1}$ and carrier concentration of $8.82 \times 10^{16} \text{ cm}^{-3}$.

1 Introduction

Photovoltaic's has emerged as an important area of energy harvesting research due to its high abundance and sustainability. Among available photovoltaic technologies, the thin film photovoltaic route found to be viable and competing with conventional technologies. To date, the most leading and promising absorber material for thin film solar cells is $\text{Cu}(\text{In,Ga})\text{Se}_2$ (CIGS) with a conversion efficiency of 22.6% [1]. However, the cost of CIGS photovoltaic devices is still high due to utilization of non-abundant In and Ga. To compensate such limitations it is required to replace the trending CIGS with an absorber material constituted of elements that are earth abundant and possessing suitable photovoltaic properties. This led the researchers focusing aim towards earth abundant absorbers like $\text{Cu}_2\text{ZnSnSe}_4$ (CZTSe), $\text{Cu}_2\text{ZnSnS}_4$ and $\text{Cu}_2\text{ZnSn}(\text{S}_x\text{Se}_{1-x})_4$ for thin films solar cells. Among them, $\text{Cu}_2\text{ZnSnSe}_4$ material has a direct optical band gap $\sim 1 \text{ eV}$ with high absorption coefficient ($> 10^4 \text{ cm}^{-1}$) and achieved a photovoltaic conversion efficiency of 11.6% [2] till date. As this achieved efficiency is still far away from theoretical efficiency of CZTSe

Electronic supplementary material The online version of this article (doi:10.1007/s10854-017-7773-x) contains supplementary material, which is available to authorized users.

✉ G. Hema Chandra
drghc@rediffmail.com

- ¹ Thin Film Laboratory, Department of Physics, Visvesvaraya National Institute of Technology, Nagpur, Maharashtra 440 010, India
- ² Energy and Health Monitoring Instrumentation Laboratory, Department of Instrumentation & Applied Physics, Indian Institute of Science, Bangalore 560 012, India
- ³ Advanced Materials Research Laboratory, Department of Physics, Yogi Vemana University, Kadapa, Andhra Pradesh 516 003, India
- ⁴ National Physical Laboratory, K. S. Krishnan Road, New Delhi 110 012, India
- ⁵ UGC-DAE Consortium for Scientific Research, Khandwa Road, Indore 452 017, India
- ⁶ Department of Materials Science and Engineering, National University of Singapore, Singapore 117576, Singapore

and incomparable with CIGS [3], a detailed study on $\text{Cu}_2\text{ZnSnSe}_4$ material is required to improve its photovoltaic performance.

Two stage process found to be preferable and very successful for growth of $\text{Cu}_2\text{ZnSnSe}_4$ films [4] due to its scalability with large throughput. In first step, metallic stacks of Cu–Zn–Sn were deposited onto glass/Mo coated glass substrate using several techniques such as co-evaporation [5], sputtering [6–12], vacuum evaporation [13], electro deposition [14–16], e-beam evaporation [17], spin coating [18] and knife edge coating [19]. Later, selenization of metallic precursors was carried out using elemental selenium/ H_2Se gas in presence of inert Ar/ N_2 atmosphere at elevated temperature (≥ 450 °C).

Although, high quality $\text{Cu}_2\text{ZnSnSe}_4$ thin films were prepared using selenization of metallic precursors at elevated temperature (≥ 450 °C), but found to contain minor secondary phases, which are affecting device performance adversely [20]. Also, poor adhesion with molybdenum coated substrates was found to be a major drawback with pure metal precursors due to the large expansion during selenization. Further, it is observed that incorporation of Se into Mo back contact increased with increase in selenization temperature (≥ 450 °C) causing transformation of Mo into MoSe_2 leading to delamination of the films, which is further detrimental to device parameters such as open circuit voltage and fill factor. Additionally, the highly resistive nature of MoSe_2 [20, 21] results in poor device performance.

To overcome the aforementioned problems associated with selenization of metal precursors at elevated temperatures, it is necessary to focus on low temperature annealing treatment utilizing precursors of metal selenides. An improvement in the adhesion was observed with the inclusion of binary selenides for growth of CuInSe_2 films [22, 23]. Since the densities of CuSe, ZnSe and SnSe are closer to $\text{Cu}_2\text{ZnSnSe}_4$, the expansion causes minor stress during the course of annealing. Although, few reports are available on preparation of CZTSe thin films using pure binary selenide [19, 24–27] precursors, but includes high temperature selenization process that too focused particularly on Glass/ZnSe/SnSe(SnSe_2)/CuSe(Cu_{2-x}Se) stacking order. As CZTSe crystallization is mainly dependent on the stacking order of precursor and further stack order is important in obtaining favorable optoelectronic properties for photovoltaic applications [28], the present investigation is aimed at utilizing a novel stacking order (SnSe/Se/CuSe/Se/ZnSe/Se/CuSe/Se) that enables low temperature selenization for realizing $\text{Cu}_2\text{ZnSnSe}_4$ thin films suitable for fabricating thin film solar cells on flexible substrates for role to role device application.

2 Experimental

$\text{Cu}_2\text{ZnSnSe}_4$ thin films were prepared using a two stage process. In the first step, deposition of multilayer precursor stack using binary selenides was carried out in high vacuum. Later, these multilayer precursor stacks were annealed in selenium atmosphere at a pressure of 100 mbar. The stacks of CuSe, ZnSe, SnSe and elemental Se (obtained from Alfa Aesar, USA) were deposited onto the ultrasonically cleaned soda lime glass substrate held at substrate temperature of 100 °C using e-beam evaporation method. A pressure of 1×10^{-5} mbar was maintained during deposition of precursor layers [SnSe/Se/CuSe/Se/ZnSe/Se/CuSe/Se] $\times 4$. The thickness of each precursor layer was chosen in such way to acquire Cu-poor and Zn-rich composition. The thickness of the precursor layers during deposition was monitored using quartz crystal thickness monitor (Model: CTM-200) and the total thickness of precursor film was found to be 580 nm.

Precursor layers were selenized inside partially opened graphite box of volume 13 cm³ with conventional thermal process using horizontal tabular furnace. The graphite box carrying precursor films and 50 mg of selenium powder was inserted into quartz tube. This graphite box was partially opened to maintain the selenium atmosphere inside it and to enable the reaction with the precursor in an inert atmosphere [10]. Initially, quartz tube was evacuated using rotary pump to a pressure of 10^{-2} mbar. Later, the temperature was increased to 170 °C, at which Ar gas was purged into quartz tube to maintain a pressure of 100 mbar. Further, the temperature was increased to 200 °C and pre-annealing treatment was conducted at this temperature for 30 min to ensure the mixing of selenium into the alloy precursor. Later, the temperature was increased to annealing temperature ranging from 250 to 450 °C and maintained at that temperature for 30 min to re-crystallize the pre-annealed film and then it was allowed to cool naturally to room temperature. Schematic diagram of preparation of $\text{Cu}_2\text{ZnSnSe}_4$ thin films using the two stage approach is shown in supplementary data.

The thickness of selenized CZTSe films were measured using Dektak XT Surface profiler (Bruker) with 12.5 μm stylus radius. The surface morphology of selenized films was examined using ULTRA55 FE-SEM Carl Zeiss MonoK1. Energy dispersive analysis of X-ray (EDAX) attached to ULTRA55 FE-SEM was used to measure the chemical composition of selenized films with an acceleration potential of 25 kV. The energy dispersive X-ray detector (EDX) was calibrated by single crystal silicon with a measurement error of ± 1 at.%. Hiden Analytical SIMS work station operated in ultrahigh vacuum with oxygen ion (Energy: 5 keV) source was used to analyze the elemental depth profile of CZTSe thin films. A BRUKER D8 advance X-ray diffractometer (XRD) with a Cu-K_α radiation source ($\lambda = 1.5406$ Å) was used to determine the structural properties of selenized

CZTSe thin films with 2θ range from 15° to 60° with a scan rate of $0.02^\circ/\text{second}$. General Structure Analysis System (GSAS) equipped with graphical user interface [29] was used for Rietveld refinement of XRD pattern. Raman spectra was recorded using Jobin Yvan LabRAM HR in backscattering configuration with different excitation laser source of wavelengths 455, 514 and 785 nm. Spectral transmittance and reflectance of the films was recorded in the wavelength range 400–2000 nm in steps of 2 nm using JASCO V-670 UV-Vis-NIR double beam spectrophotometer. Electrical properties of the films at room temperature were determined using a Hall effect measurement (ECOPIA HMS-3000) with an applied magnetic field of 1 T and a current of 0.1 mA.

3 Results and discussion

3.1 Compositional analysis

The chemical composition of the multiple stacks selenized at different temperatures were quantitatively measured using energy dispersive X-ray spectroscopy. The measurements were carried out at different locations for each film and are found to be homogeneous throughout the film and their mean values are presented in Table 1. It is observed that, the composition of $\text{Cu}_2\text{ZnSnSe}_4$ thin films significantly depends on selenization temperature. With an increase in selenization temperature of films from 250°C to 450°C , the Zn/Sn, Cu/(Zn + Sn) and Se/(Cu + Zn + Sn) ratios are found to vary between 0.97 and 6.07, 0.7–0.85 and 1.20–0.76, respectively. The multiple stacks selenized below 350°C have shown Cu deficiency and excess Sn and Se in the composition. The composition of multiple stacks selenized at a temperature of 350°C was found to be slightly Cu-poor and Zn-rich and the estimated atomic percentages for copper, zinc, tin and selenium were 21.82, 14.03, 12.31 and 51.84, respectively. While the films selenized above 350°C shows significant loss of Sn and Se and is attributed to re-evaporation of SnSe_x ($x = 1$ or 2) and Se.

The SIMS depth profile of multiple stacks selenized at a temperature of 350°C is shown in Fig. 1. It is observed that the distribution of Cu, Sn and Se found to be homogeneous

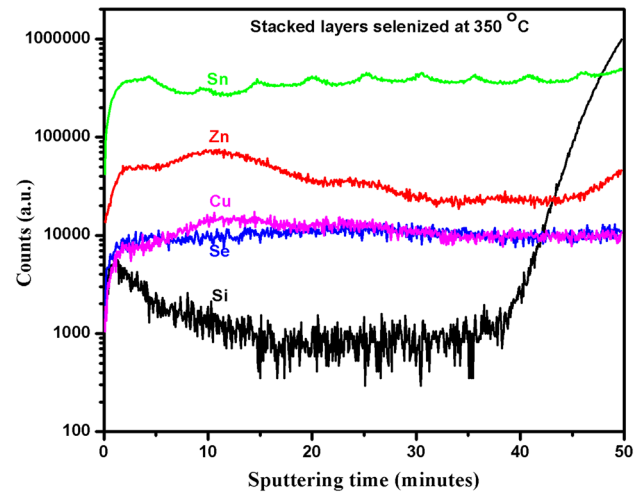


Fig. 1 SIMS depth profiles of precursor stacks selenized at 350°C

across the thickness of the film, whereas Zn content appeared relatively more in the top portion of the film indicating the out diffusion of Zn. Comprehensively, the distribution of all the constituent elements are found to be uniform for the multiple stacks selenized at a temperature of 350°C .

3.2 Structural analysis

The selenization temperature (T_{Se}) was found to have significant influence on the structure of the films. Figure 2 shows the XRD pattern of multiple stacks selenized at various temperatures. From XRD pattern, it is observed that all the selenized precursor stacks are polycrystalline in nature. The precursor stacks selenized at a temperature of 250°C shows the XRD peaks at 2θ values of 27.31° , 45.16° and 53.51° reveals the formation of ternary Cu_2SnSe_3 phase (monoclinic) along with ZnSe phase (hexagonal). The pre-annealing treatment at 200°C and subsequent selenization at 250°C found to be favourable for reaction between CuSe and SnSe to form ternary Cu_2SnSe_3 phase. The XRD pattern of precursor stacks selenized at a temperature of 300°C shows the peaks at 2θ values of 27.21° , 45.24° and 53.53° . The shift in dominant peak (112) towards slightly lower 2θ value (27.21°) reveals

Table 1 Elemental composition of CZTSe thin films determined from EDX analysis

T_{Se} ($^\circ\text{C}$)	Cu (at.%)	Zn (at.%)	Sn (at.%)	Se (at.%)	$\frac{\text{Zn}}{\text{Sn}}$	$\frac{\text{Cu}}{(\text{Zn}+\text{Sn})}$	$\frac{\text{Se}}{(\text{Cu}+\text{Zn}+\text{Sn})}$	Thickness (nm)
250	18.79	13.13	13.42	54.66	0.97	0.70	1.20	950
300	20.16	13.68	13.04	53.12	1.04	0.75	1.13	880
350	21.82	14.03	12.31	51.84	1.13	0.82	1.07	810
400	22.89	16.82	10.93	49.36	1.53	0.82	0.97	760
425	24.68	19.69	9.17	46.46	2.14	0.85	0.86	585
450	26.10	26.32	4.33	43.25	6.07	0.85	0.76	440

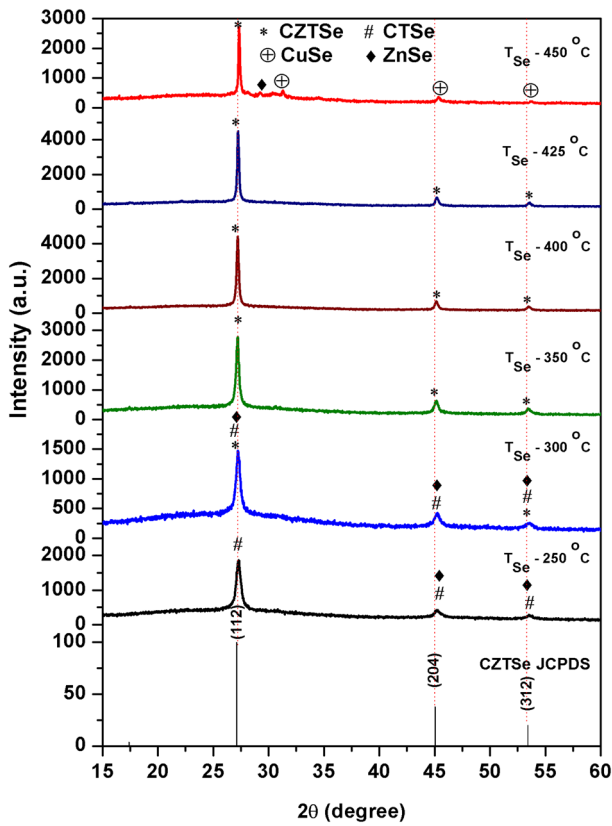


Fig. 2 XRD pattern of precursor stacks selenized at different temperatures

the initiation of $\text{Cu}_2\text{ZnSnSe}_4$ phase formation. However, the existence of ternary Cu_2SnSe_3 and binary ZnSe phase cannot be confirmed solely by XRD measurements, since the 2θ values corresponding to $\text{Cu}_2\text{ZnSnSe}_4$, Cu_2SnSe_3 and ZnSe phases are very similar to each other.

The diffraction peaks observed at 2θ values of 27.21° , 45.15° and 53.41° for multiple stacks selenized at 350°C are corresponding to (112), (204) and (312) planes of tetragonal $\text{Cu}_2\text{ZnSnSe}_4$ (JCPDS # 52-0868). The grown $\text{Cu}_2\text{ZnSnSe}_4$ thin films shows (112) plane as a strong preferred orientation and no secondary phases are observed, which is further verified by Raman spectroscopy. The formation of single phase $\text{Cu}_2\text{ZnSnSe}_4$ thin films at a selenization temperature of 350°C is attributed to thermally induced enhancement in the chemical kinetics of overall reaction, which results in complete reaction between ternary and binary selenide results in formation of quaternary $\text{Cu}_2\text{ZnSnSe}_4$ compound film. Rietveld refinement was performed for the XRD patterns of multiple stacks selenized at 350°C (shown in supplementary data) using GSAS to further confirm the structure. Rietveld refinement of the XRD pattern for the CZTSe films selenized at 350°C shows an $\text{Rwp}=3.74$ with goodness of fit $\chi^2=1.022$. The lattice parameters of $\text{Cu}_2\text{ZnSnSe}_4$ found to be $a=5.695(1)\text{ \AA}$, $c=11.334(4)\text{ \AA}$ with a space group of I4,

which are in accordance with the values reported in literature [29]. From XRD data ($c/2a \sim 1$), diffraction peaks and lattice constants it is confirmed that the multiple stacks selenized at a temperature of 350°C has a kesterite structure [30]. Single phase was observed for the precursor stacks selenized at a temperature of 350°C in spite of minor deviation in composition is attributed to the self-assessing tendency of $\text{Cu}_2\text{ZnSnSe}_4$ films [31]. To the best of our knowledge, none of the group has reported low temperature crystallization of $\text{Cu}_2\text{ZnSnSe}_4$ thin films using stacked precursors. The texture coefficients for different crystal planes were calculated for the CZTSe film selenized at 350°C from XRD data using the following Eq. (1)

$$TC_{(hkl)} = \frac{I_{(hkl)}}{I_{0(hkl)}} \quad (1)$$

$$= \frac{1}{n} \sum_{(hkl)} \left(\frac{I_{(hkl)}}{I_{0(hkl)}} \right)$$

where TC is the texture coefficient of the corresponding (hkl) plane, $I_{(hkl)}$ is the measured intensity of the (hkl) reflex, $I_{0(hkl)}$ is the intensity of the same reflex in the reference diffraction pattern which is considered as a completely random oriented sample, and n is the reflection number [32]. The calculated texture coefficients of (112), (220) and (312) planes were 1.40, 0.76 and 0.83 respectively, which strongly corroborates the preferred orientation along (112) plane.

The multiple stacks selenized at the temperatures of 400 and 425°C shows a trend similar to that of films selenized at 350°C . However, 2θ values of films grown at selenization temperature of 425°C are slightly shifted towards higher angle is attributed to defect formation in the films due to re-evaporation of volatile elements such as Sn and Se. The selenized precursor stacks at 450°C shows peaks at 27.35° related to (112) orientation of $\text{Cu}_2\text{ZnSnSe}_4$ phase along with an additional peaks at 29.19° associated with ZnSe Phase (JCPDS # 89-2940). In addition to this, the peaks at 2θ values 31.23° , 45.34° and 53.70° are observed corresponding to CuSe (hexagonal) phase (JCPDS # 34-0171). Hence, XRD pattern of precursor stacks selenized at a temperature of 450°C reveals the decomposition of quaternary $\text{Cu}_2\text{ZnSnSe}_4$ phase into CuSe and ZnSe phases.

3.3 Raman spectroscopy

It is very difficult to confirm the formation of single phase $\text{Cu}_2\text{ZnSnSe}_4$ solely from XRD analysis, since the characteristic XRD peaks of $\text{Cu}_2\text{ZnSnSe}_4$ phase overlaps with the peaks of Cu_2SnSe_3 and ZnSe . Raman spectroscopy was used as a complementary tool to distinguish and ensure the formation of $\text{Cu}_2\text{ZnSnSe}_4$ phase. Raman spectra obtained using an excitation wavelength of 514 nm for multiple stacks selenized at different temperatures are shown in Fig. 3a. The

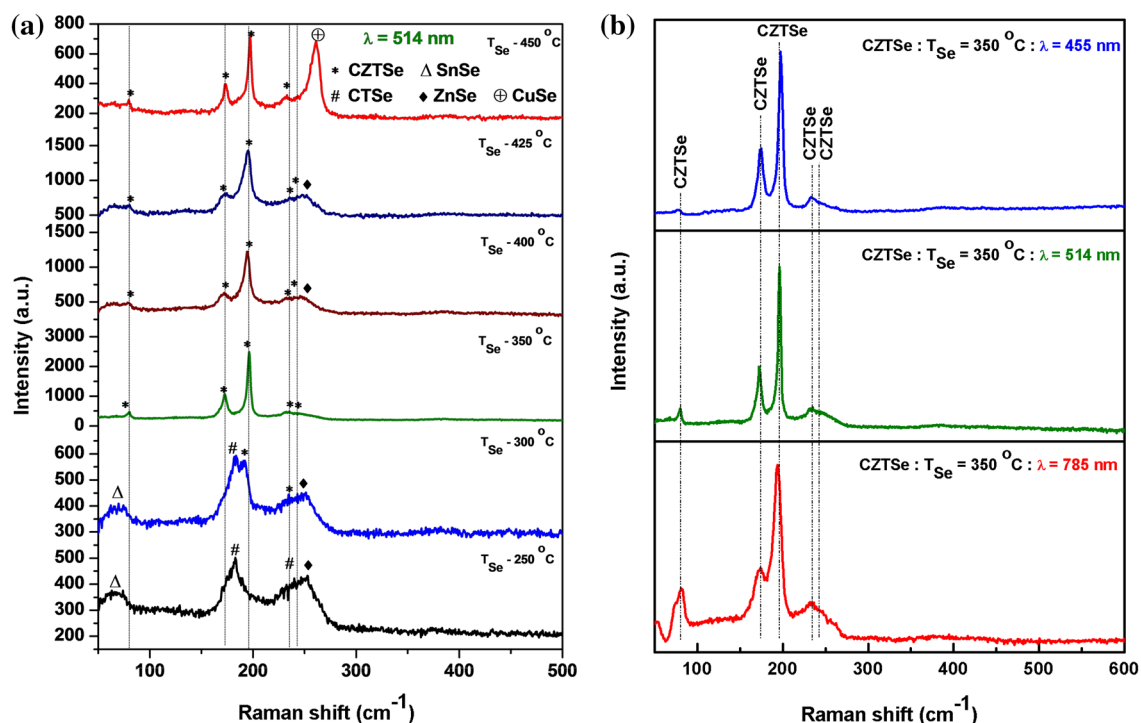


Fig. 3 **a** Raman spectra of the precursor stacks selenized at different temperatures. **b** Multi wavelength Raman spectra of CZTSe thin films selenized at 350 °C

precursor's selenized at a temperature of 250 °C shows the broad and less intense Raman peaks at 67, 183, 232 and 253 cm^{-1} . A minor peak at 67 cm^{-1} is associated with SnSe (orthorhombic) phase [33] and other two peaks at 183 and 232 cm^{-1} can be attributed to ternary Cu_2SnSe_3 phase [34]. A peak at 183 cm^{-1} relates with both Cu_2SnSe_3 and SnSe_2 phase. However, no signature of SnSe_2 was observed in XRD measurement and hence concluded that it belongs to Cu_2SnSe_3 and the formation of SnSe_2 phase can be ruled out. The Raman peak located at 253 cm^{-1} is attributed to ZnSe phase [34]. The multiple stacks selenized at a temperature of 300 °C show the Raman modes at 67, 184, 192, 234 and 251 cm^{-1} . The broad and asymmetric peaks at 67, 184 and 251 cm^{-1} shows the presence of SnSe, Cu_2SnSe_3 and ZnSe phases respectively, while the peaks at 192 and 234 cm^{-1} are associated with $\text{Cu}_2\text{ZnSnSe}_4$ phase. Hence, the Raman spectra reveal the selenization of precursor stacks at 300 °C is a pre-mature growth of $\text{Cu}_2\text{ZnSnSe}_4$ phase formation.

The well-defined Raman spectra was observed for multiple stacks selenized at a temperature of 350 °C with peaks at 80, 172, 196, 234 and 244 cm^{-1} that corresponds to single phase $\text{Cu}_2\text{ZnSnSe}_4$. The two Raman modes at 172 cm^{-1} (A symmetry) and 196 cm^{-1} (A symmetry) are well distinguished and symmetrical in nature. In addition to this, the peaks are observed to be sharp and intense which confirms the formation of highly crystalline and pure kesterite $\text{Cu}_2\text{ZnSnSe}_4$ phase.

Similar trend was observed for $\text{Cu}_2\text{ZnSnSe}_4$ thin films grown at selenization temperatures 400 and 425 °C, however the peaks are relatively broad and asymmetric in nature which is attributed to the lattice defect induced phonon confinement, low crystallinity, presence of strain and local composition deviation in the films [35]. Furthermore, both the films show an additional Raman mode at $\sim 250 \text{ cm}^{-1}$ corresponding to ZnSe phase, which is due to re-evaporation of volatile SnSe phase at elevated temperatures resulted in accumulation of ZnSe phase at the surface [36]. The multiple stacks selenized at a temperature of 450 °C shows relatively low intense Raman modes of $\text{Cu}_2\text{ZnSnSe}_4$ phase at 80, 173, 197 and 233 cm^{-1} with an additional sharp peak at 261 cm^{-1} revealing the presence of CuSe phase [34], as evident from XRD analysis. The observation of CuSe phase at selenization temperature 450 °C clearly indicates phase separation due to the re-evaporation of volatile elements as supplemented by EDX analysis. Full width at half maximum (FWHM) value corresponding to Raman peak at 196 cm^{-1} for the film selenized at temperature 350 °C found to be narrow (3.20 cm^{-1}) compared to the films selenized at temperature 400 °C (5.31 cm^{-1}) and 425 °C (12.99 cm^{-1}) revealing improved crystallinity and minimal defects.

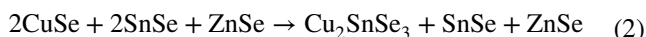
Usually, for structural studies, micro Raman spectroscopy measurements are carried out with the use of green excitation wavelength of 514 or 532 nm. The excitation with green wavelength may limit the identification of undesirable

secondary phases thereby it requires the use of different excitation wavelengths leading to near resonant excitation conditions for certain secondary phases which enables the detection of weak modes due to enhancement in the peak intensity [37]. There is a possibility that the secondary phases like SnSe₂ and ZnSe may remain undetected despite the usual green Raman and XRD analysis has shown single Cu₂ZnSnSe₄ phase for the film selenized at 350 °C. To ensure the phase purity concluded by XRD analysis and Raman spectroscopy with an excitation wavelength of 514 nm, multiple wavelength Raman measurements were carried out for the precursor stacks selenized at 350 °C. The Raman spectra observed with multi-excitation wavelengths (455, 514 and 785 nm) are depicted in Fig. 3b. Raman spectra shows peaks corresponding to Cu₂ZnSnSe₄ phase only for all the three excitation wavelengths with no traces of secondary phases which corroborates the phase purity of Cu₂ZnSnSe₄ thin films selenized at 350 °C.

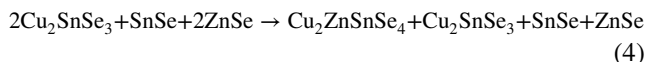
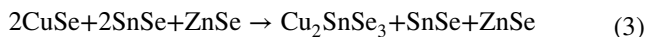
3.4 Reaction mechanism

It is observed that the pre-annealing treatment, novel stacking order and thickness of each layer has enabled the formation of single phase Cu₂ZnSnSe₄ at lower selenization temperature. Based on XRD and Raman analysis the reaction paths for formation of binary, ternary and quaternary phases at different selenization temperature were presented.

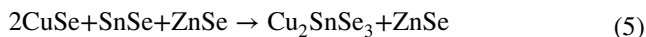
- (1) It is well known that, CuSe react more quickly with SnSe than other copper selenides phases (CuSe₂, Cu_{2-x}Se). At lower selenization temperature (T_{se} = 250 °C), CuSe reacts with SnSe and form ternary Cu₂SnSe₃ phase. Hence, the presence of Cu₂SnSe₃, SnSe and ZnSe are detected.



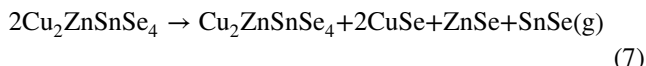
- (2) Cu₂SnSe₃ reacts with ZnSe to form Cu₂ZnSnSe₄ phase at the selenization temperature (T_{se}) of 300 °C. But it is observed that, selenization temperature was insufficient to complete formation of single phase Cu₂ZnSnSe₄. An incomplete conversion of binaries into ternary/quaternary phases were observed due to the deficiency of CuSe.



- (3) At T_{se} = 350 °C, Cu₂SnSe₃ and ZnSe were found to react completely with each other and resulted in single phase Cu₂ZnSnSe₄.

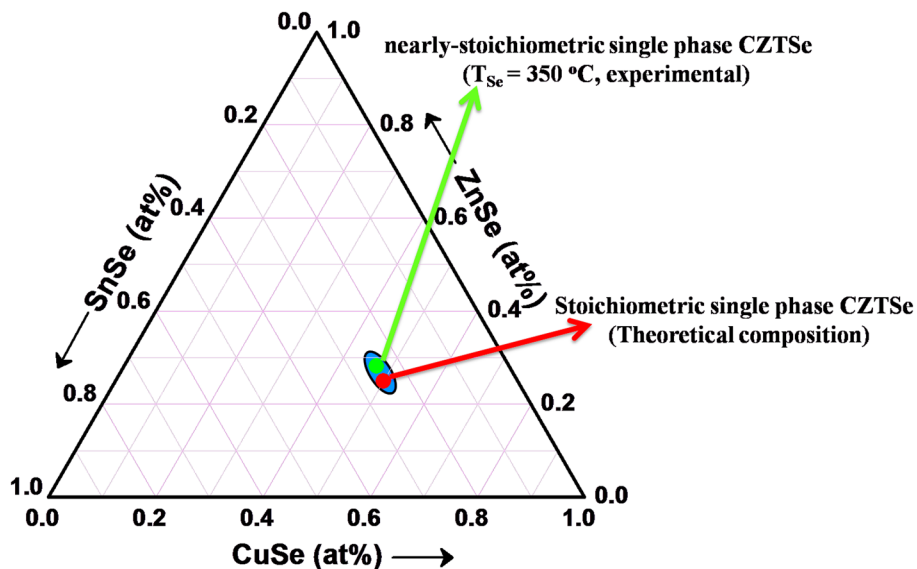


- (4) At higher selenization temperature (T_{se} = 450 °C), due to the re-evaporation of SnSe decomposition of Cu₂ZnSnSe₄ phase take place, resulting into binary CuSe and ZnSe phase along with Cu₂ZnSnSe₄ phase.



The quasi-ternary phase diagram of the CuSe–ZnSe–SnSe system is shown in Fig. 4, which depict nearly-stoichiometric composition for single-phase Cu₂ZnSnSe₄ measured using EDX (green spot). The stoichiometric composition

Fig. 4 Quasi-ternary phase diagram of the CuSe–ZnSe–SnSe system



for single-phase $\text{Cu}_2\text{ZnSnSe}_4$ was shown by red colour in the phase diagram. From phase diagram, it is observed that CuSe-ZnSe-SnSe system exhibits very small region (blue spot) of stability for single-phase kesterite $\text{Cu}_2\text{ZnSnSe}_4$ thin films. Furthermore, the process of formation of single-phase $\text{Cu}_2\text{ZnSnSe}_4$ is self limiting and small deviation in composition results in the formation of various binary and ternary phases. Hence, it is required to control composition systematically.

3.5 Surface morphology

The FESEM micrographs of multiple stacks selenized at temperatures of 250, 350, 425 and 450 °C are shown in Fig. 5. The FESEM image of multiple stacks selenized at a temperature of 250 °C shows small sized cylindrical grains (length \sim 200 nm), which are uniformly distributed throughout the surface of substrate. With an increase in selenization temperature of $\text{Cu}_2\text{ZnSnSe}_4$ thin films from 250 to 350 °C, the small sized cylindrical grains grown bigger. The grains have clear cylindrical shape of length \sim 425 nm. In addition to this, white granules of very small size (few nanometers) are anchored on the surface of the $\text{Cu}_2\text{ZnSnSe}_4$ thin films. To confirm the composition of tiny granules, the elemental

mapping was carried out using EDX for multiple stacks selenized at a temperature of 350 °C and results are shown in supplementary data. The elemental mapping showing a uniform distribution of constituent elements on the surface with no colour contrast that rules out the segregation of spurious binary phases on to surface. The deformation was clearly observed at the edges of grains from the micrographs of multiple stacks selenized at a temperature of 425 °C indicating an increase in the defect density arise due to decomposition of compound. Furthermore, the agglomeration of grains has been observed for stacked layers selenized at a temperature of 450 °C and large voids are present in-between the grains, which may be due to the re-evaporation of volatile elements at elevated temperature results in decomposition of quaternary $\text{Cu}_2\text{ZnSnSe}_4$ phase into secondary phases. The cross sectional SEM images of the stacked layers selenized at temperature 250, 350 and 425 °C are shown in supplementary data. The cross sectional SEM of $\text{Cu}_2\text{ZnSnSe}_4$ films selenized at 250 °C shows loosely packed grains with cauliflower like morphology. Whereas, the films selenized at a temperature of 350 °C show compact and larger grains. A further increase in selenization temperature to 425 °C led to a sign of slight delamination between the multi-layers structures.

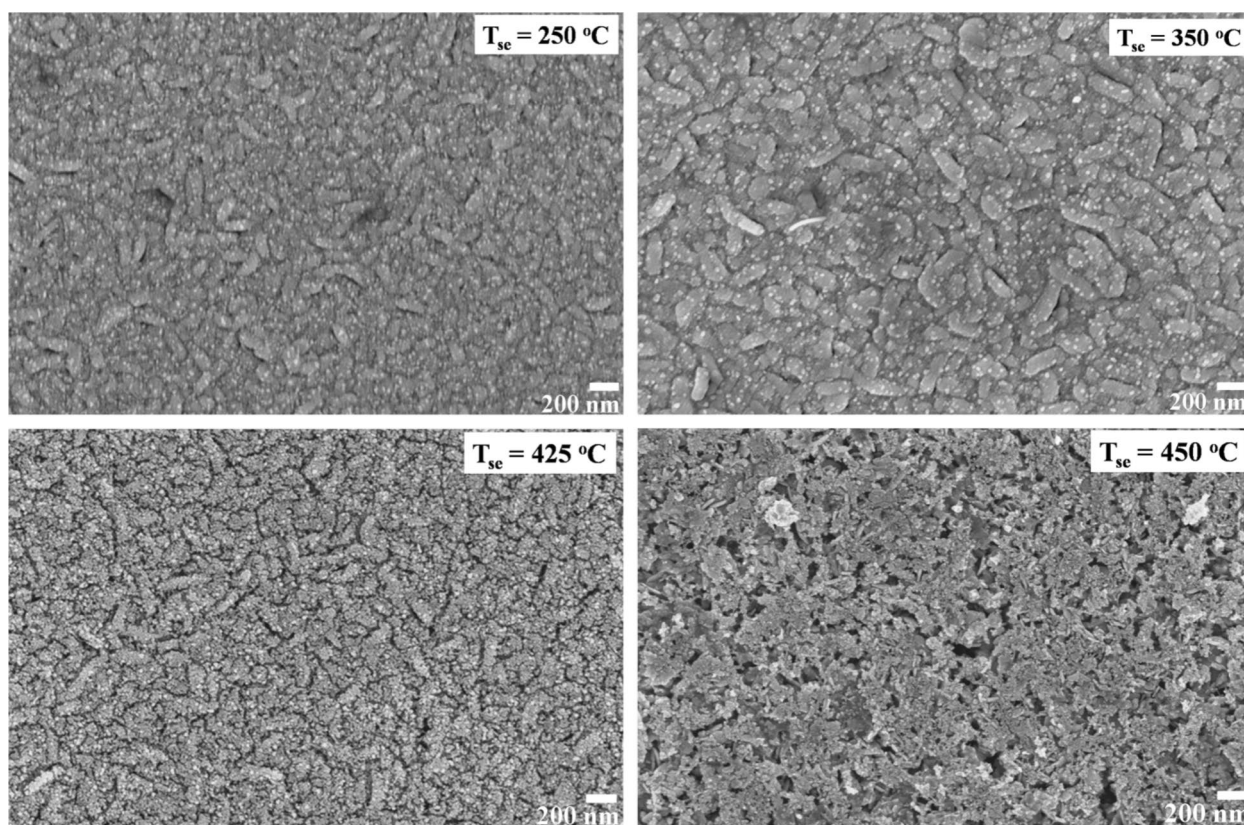


Fig. 5 FESEM images of the stacked layers selenized at 250, 350, 425 and 450 °C

3.6 Optical properties

Figure 6a and b shows the optical transmittance and reflectance spectra of multiple stacks selenized at different temperatures from 250 to 450 °C. The transmittance spectra of selenized stacked layers reveal that there are considerable deviations in transmittance spectra close to the absorption edge with an increase in selenization temperature. The stacked layers selenized at 250 °C shows low spectral transmittance of 15%, while transmittance of 25–50% was observed nearer to absorption edges of the films selenized at temperatures 300, 350 and 400 °C. An oscillatory behavior observed at ~1600 nm for stacked layers selenized at 300, 350 and 400 °C were caused by interference due the difference in refractive index of Cu₂ZnSnSe₄ film and the glass substrate. An enhancement in the optical transmittance for multiple binary selenide stacks selenized at 300, 350 and 400 °C indicating a sign of an increase in grain size with less grain boundaries results in decreasing scattering of photons

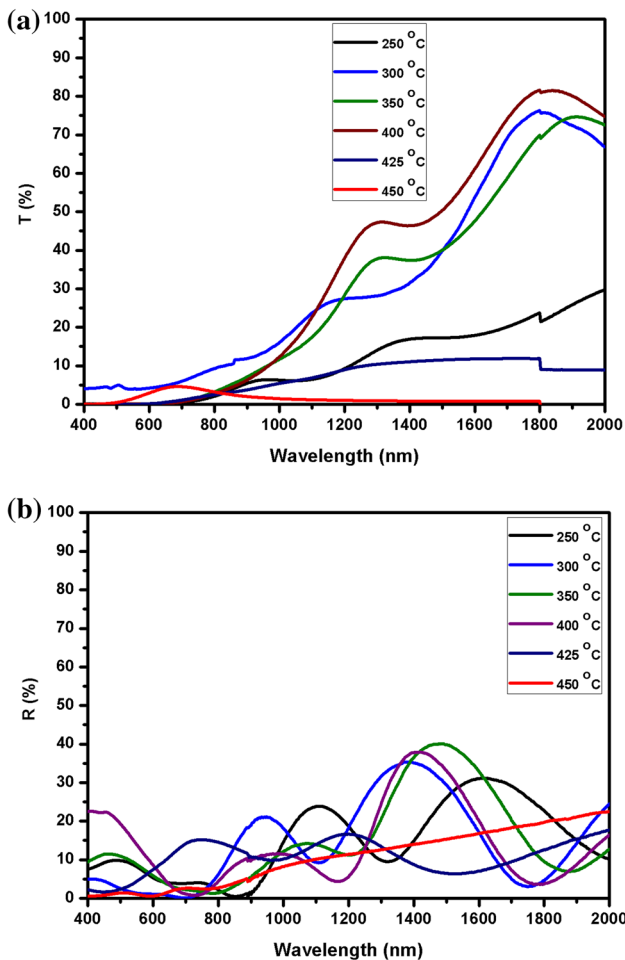


Fig. 6 **a** The optical transmittance spectra of precursor layers selenized at different temperatures. **b** The optical reflectance spectra of precursor layers selenized at different temperatures

[38]. Similarly, the sharpness observed in the interference fringes of stacked layers selenized at 300, 350 and 400 °C indicates a decrease of surface roughness with improvement in the film crystallinity [39]. A low transmittance (less than 10%) was observed for stacked layers selenized at a temperature of 450 °C due to the poor crystallinity [40]. The appearance of maxima and minima in reflectance spectra indicates the specular nature of selenized thin films, thus revealing negligible possibility of scattering [41]. The optical absorption coefficient (α) is calculated using spectral transmittance (T) and reflectance (R) data with the help of Eq. 8 [34].

$$\alpha = -\frac{1}{t} \ln \left[\frac{-(1-R)^2 + \sqrt{(1-R)^4 + 4T^2R^2}}{2TR^2} \right] \quad (8)$$

where ‘t’ is the thickness of the film. The nature of the optical transition and the optical band gap for each film is obtained from Eq. 9,

$$\alpha h\nu = A(h\nu - E_g)^n \quad (9)$$

where A is constant. The values of ‘ α ’ are found to obey Eq. (9) for $n=1/2$, suggesting that the optical transitions are direct-allowed. The optical band gap was determined by extrapolating the linear region of the plot $(\alpha h\nu)^2$ versus $h\nu$ and taking the intercept at $\alpha=0$.

Figure 7a show the plots of $(\alpha h\nu)^2$ versus $h\nu$ for the multiple stacks selenized at temperatures 250, 350 °C and Fig. 7b shows the plot of film selenized at 450 °C. It can be seen from Fig. 7a that the energy gap of stacked layers selenized at a temperature of 250 °C was found to be 0.81 eV, thereby confirms the formation of ternary phase (Cu₂SnSe₃). Even though signatures of ZnSe phase were observed from XRD and Raman analysis, no traces of it (ZnSe phase) were detected from transmittance spectrum and this is attributed to limitations associated with low spectral intensity as the fundamental edge falls below 600 nm. The optical band gap of 1.01 eV was observed for precursor stacks selenized at a temperature 350 °C indicating the formation of single phase Cu₂ZnSnSe₄ as evident from XRD and Raman analysis. Also, it is in good agreement with reported literature [9, 11]. The Cu₂ZnSnSe₄ thin film selenized at temperature 450 °C shows higher band gap of 1.85 eV might be due to the presence of secondary CuSe phase [42] in the film that has reflected in XRD and Raman spectra.

3.7 Electrical properties

The effect of selenization temperatures on the electrical properties of Cu₂ZnSnSe₄ thin films was studied using Hall Effect set up at room temperature. Despite of variation in selenization temperature, all films shows p-type conductivity indicating the presence of intrinsic point defects in the grown films. The electrical properties of multiple stacks

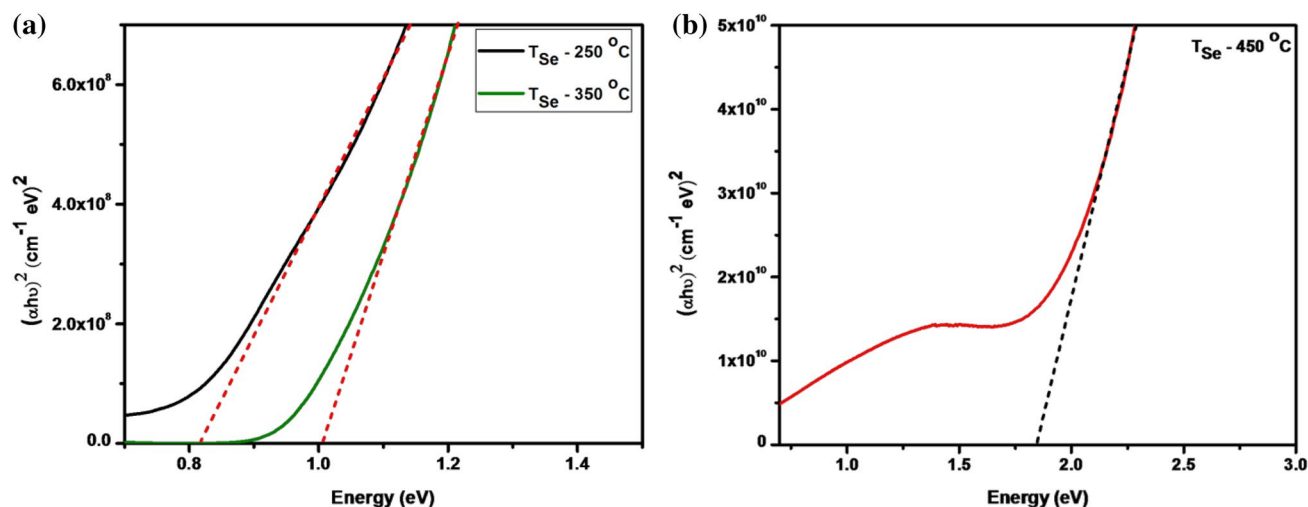


Fig. 7 **a** Plot of $(\alpha h\nu)^2$ versus $h\nu$ for precursor stacks selenized at 250 and 350 °C. **b** Plot of $(\alpha h\nu)^2$ versus $h\nu$ for precursor stacks selenized at 450 °C

Table 2 Electrical properties of stacked layers selenized at different temperatures

Selenization temperature (°C)	Resistivity (Ω cm)	Mobility ($\text{cm}^2(\text{Vs})^{-1}$)	Carrier concentration (cm^{-3})
250	1.78×10^{-1}	4.96×10^{-1}	7.02×10^{19}
300	1.25	3.04	1.63×10^{18}
350	4.66	15.17	8.82×10^{16}
400	2.60×10^{-1}	3.41×10^{-1}	7.03×10^{19}
425	1.41×10^{-2}	5.11×10^{-2}	8.62×10^{21}
450	8.55×10^{-2}	1.32×10^{-2}	5.49×10^{21}

selenized at various temperatures are shown in Table 2. The multiple stacks selenized at a temperature of 250 °C shows low resistivity due to the presence of ternary $\text{Cu}_2\text{ZnSnSe}_3$ phase. Further increase in selenization temperature from 250 to 350 °C has resulted in improvement of Hall mobility from 4.96×10^{-1} to $15.17 \text{ cm}^2(\text{Vs})^{-1}$. The increase in selenization temperature led to reduce the defects and improve the phase purity and uniformity in composition of the $\text{Cu}_2\text{ZnSnSe}_4$ films causing enhancement in the mobility. It is observed from FESEM image that with an increase in selenization temperature from 250 to 350 °C the grain sizes are also found to be increased which has reduced the grain boundary scattering of carriers thereby enhanced the hole mobility. The values of electrical resistivity, mobility and carrier concentration for $\text{Cu}_2\text{ZnSnSe}_4$ films selenized at temperature 350 °C were found to be 4.66Ω cm, $15.17 \text{ cm}^2(\text{Vs})^{-1}$ and $8.82 \times 10^{16} \text{ cm}^{-3}$ respectively, which are in good agreement with reported values [31, 43]. $\text{Cu}_2\text{ZnSnSe}_4$ films selenized at a temperature of 450 °C shows high carrier concentration $5.49 \times 10^{21} \text{ cm}^{-3}$ with mobility $1.32 \times 10^{-2} \text{ cm}^2(\text{Vs})^{-1}$ and

resistivity $8.55 \times 10^{-2} \Omega$ cm, which may be due to the presence of secondary CuSe phase and the decreased grain size as evident from XRD and FESEM results.

4 Conclusions

The high quality $\text{Cu}_2\text{ZnSnSe}_4$ films were successfully prepared onto soda lime glass substrates by low temperature selenization of e-beam evaporated multiple binary selenide precursor stacks. The effect of selenization temperature on the physical properties of $\text{Cu}_2\text{ZnSnSe}_4$ thin films was systematically studied. The $\text{Cu}_2\text{ZnSnSe}_4$ thin films selenized at different temperatures are found polycrystalline in nature. The $\text{Cu}_2\text{ZnSnSe}_4$ film grown at selenization temperature 350 °C exhibited kesterite structure having lattice parameters $a = 5.695$ (1) Å, $c = 11.334$ (4) Å with (112) preferred orientation. Raman measurement using multi-wavelength excitation confirms the grown films were single phase $\text{Cu}_2\text{ZnSnSe}_4$. The compositional analysis revealed that the obtained films are slightly Cu-poor and Zn-rich. The optical absorption studies indicated a direct band gap of 1.01 eV. The $\text{Cu}_2\text{ZnSnSe}_4$ film selenized at 350 °C showed *p*-type conductivity with electrical resistivity of 4.66 Ω cm, mobility of $15.17 \text{ cm}^2(\text{Vs})^{-1}$ and carrier concentration of $8.82 \times 10^{16} \text{ cm}^{-3}$. The crystallization of $\text{Cu}_2\text{ZnSnSe}_4$ thin films at low temperature (350 °C) is attributed to the utilization of novel multiple binary selenide precursor stacks followed by the pre-annealing treatment at 200 °C. The grains are observed to be relatively small in size, therefore further improvement is necessary which is subjected to execute as future work.

Acknowledgements The authors are thankful to the SERB, Govt. of India, for providing financial support for establishing research laboratory to carry out the present research work through a sanctioned project (SR/S2/CMP-63/2012). We are grateful to UGC-DAE-CSR, Indore, for providing financial support (CSR-IC/CRS-83/2014-15/590) to carry out the present work and also for extending sophisticated characterization facilities for present investigation.

Compliance with ethical standards

Conflict of interest The authors have no conflict of interest to declare.

References

- P. Jackson, R. Wuerz, D. Hariskos, E. Lotter, W. Witte, M. Powalla, *Phys. Status Solidi Rapid Res. Lett.* **10**, 583 (2016)
- Y.S. Lee, T. Gershon, O. Gunawan, T.K. Todorov, T. Gokmen, Y. Virgus, S. Guha, *Adv. Energy Mater.* **5**, 2 (2015)
- W. Shockley, H.J. Queisser, *J. Appl. Phys.* **32**, 510 (1961)
- S. Oueslati, G. Brammertz, M. Buffière, H. ElAnzeery, O. Touayar, C. Köble, J. Bekaert, M. Meuris, J. Poortmans, *Thin Solid Films* **582**, 224 (2014)
- S.M. Lee, Y.S. Cho, *J. Alloys Compd.* **579**, 279 (2013)
- K.H. Kim, I. Amal, *Electron. Mater. Lett.* **7**, 225 (2011)
- H. Yoo, R.A. Wibowo, A. Hölzing, R. Lechner, J. Palm, S. Jost, M. Gowtham, F. Sorin, B. Louis, R. Hock, *Thin Solid Films* **535**, 73 (2013)
- R. Bodeux, F. Mollica, S. Delbos, *Sol. Energy Mater. Sol. Cells* **132**, 67 (2015)
- P.M.P. Salomé, P.A. Fernandes, A.F. Da Cunha, J.P. Leitão, J. Malaquias, A. Weber, J. C. González, M. I. N. Da Silva, *Sol. Energy Mater. Sol. Cells* **94**, 2176 (2010)
- A. Fairbrother, M. Neuschitzer, E. Saucedo, A. Pérez-Rodríguez, *Phys. Status Solidi Appl. Mater. Sci.* **212**, 109 (2015)
- F. Luckert, D.I. Hamilton, M.V. Yakushev, N.S. Beattie, G. Zoppi, M. Moynihan, I. Forbes, A.V. Karotki, A.V. Mudryi, M. Grossberg, J. Krustok, R.W. Martin, *Appl. Phys. Lett.* **99**, 62104 (2011)
- L.G.C. Stroth, M.H. Sayed, M. Schuster, J. Ohland, I. Hammer-Riedel, M.S. Hammer, P. Wellmann, J. Parisi, *J. Mater. Sci.* **28**, 7730 (2017)
- O. Volobujeva, J. Raudoja, E. Mellikov, M. Grossberg, S. Bereznev, R. Traksmas, *J. Phys. Chem. Solids* **70**, 567 (2009)
- L. Guo, Y. Zhu, O. Gunawan, T. Gokmen, V.R. Deline, S. Ahmed, L.T. Romankiw, H. Deligianni, *Prog. Photovoltaics Res. Appl.* **22**, 58 (2014)
- R. Juškeenas, G. Niaura, Z. Mockus, S. Kanapeckaitė, R. Giraitis, R. Kondrotas, A. Naujokaitis, G. Stalnionis, V. Pakštas, V. Karpavičiene, *J. Alloys Compd.* **655**, 281 (2016)
- Y. Zhang, C. Liao, K. Zong, H. Wang, J. Liu, T. Jiang, J. Han, G. Liu, L. Cui, Q. Ye, H. Yan, W. Lau, *Sol. Energy* **94**, 1 (2013)
- H.-Y. Huang, S.-E. Liu, *Eur. Phys. J. Appl. Phys.* **64**, 30302 (2013)
- Y. Liu, D.K. Hui, Y.C. Chen, *J. Mater. Sci.* **24**, 529 (2013)
- C.M. Fella, A.R. Uhl, Y.E. Romanyuk, A.N. Tiwari, *Phys. Status Solidi Appl. Mater. Sci.* **209**, 1043 (2012)
- O. Volobujeva, E. Mellikov, S. Bereznev, J. Raudoja, A. Öpik, T. Raadik, *Mater. Challenges Altern. Renew. Energy* **224**, 257 (2011)
- B. Shin, Y. Zhu, N.A. Bojarczuk, S. Jay Chey, S. Guha, *Appl. Phys. Lett.* **101**, 053903 (2012)
- Y.C. Lin, Y.T. Hsieh, C.M. Lai, H.R. Hsu, *J. Alloys Compd.* **661**, 168 (2016)
- S. Zweigart, *J. Cryst. Growth* **146**, 233 (1995)
- V. Alberts, S. Zweigart, H.W. Schock, *Semicond. Sci. Technol.* **217**, 217 (1997)
- R. Munir, G.S. Jung, Y.M. Ko, B.T. Ahn, *Korean J. Mater. Res.* **23**, 183 (2013)
- O. Volobujeva, E. Mellikov, K. Timmo, M. Danilson, S. Bereznev, *J. Renew. Sustain. Energy* **5**, 1 (2013)
- O. Volobujeva, S. Bereznev, J. Raudoja, K. Otto, M. Pilvet, E. Mellikov, *Thin Solid Films* **535**, 48 (2013)
- A. Fairbrother, L. Fourdrinier, X. Fontané, V. Izquierdo-Roca, M. Dimitrievska, A. Pérez-Rodríguez, E.S. Saucedo, *J. Phys. Chem. C* **118**(31), 17291 (2014)
- E. Brian, H. Toby, *J. Appl. Cryst.* **34**, 210 (2001)
- G. Suresh Babu, Y.B. Kishore Kumar, P. Uday, S. Bhaskar, S. Raja Vanjari, *J. Phys. D. Appl. Phys.* **41**, 205305/1 (2008)
- D.H. Kuo, J.T. Hsu, A.D. Saragih, *Mater. Sci. Eng. B* **186**, 94 (2014)
- M.H. Chao Gao, T. Schnabel, Tobias Abzieher, Erik Ahlswede, Michael Powalla, *Appl. Phys. Lett.* **108**, 13901 (2016)
- A. Fairbrother, X. Fontané, V. Izquierdo-Roca, M. Placidi, D. Sylla, M. Espindola-Rodríguez, S. López-Mariño, F.A. Pulgarín, O. Vigil-Galan, A.P. Rodríguez, E. Saucedo, *Prog. Photovolt. Res. Appl.* **22**, 479 (2014)
- P.M.P. Salome, P.A. Fernandes, J.P. Leitao, M.G. Sousa, J.P. Teixeira, A.F. Da Cunha, *J. Mater. Sci.* **49**, 7425 (2014)
- R. Djemour, A. Redinger, M. Mousel, L. Gütay, X. Fontané, V. Izquierdo-Roca, A. Pérez-Rodríguez, S. Siebentritt, *Opt. Exp.* **21**(Suppl 4), A695 (2013)
- Y. Hwang, B. Park, B. Lee, J.Y. Kim, J. Jeong, H. Kim, M.J. Ko, B. Kim, H.J. Son, S.Y. Lee, J. Lee, J. Park, S. Cho, D. Lee, *J. Phys. Chem. C* **118**, 27657 (2014)
- M. Dimitrievska, A. Fairbrother, X. Fontané, T. Jawhari, V. Izquierdo-Roca, E. Saucedo, A. Pérez-Rodríguez, *Appl. Phys. Lett.* **104**, (2014)
- C. Adel, B.M. Fethi, B. Brahim, *J. Mater. Sci.* **27**, 3481 (2016)
- G.G. Rusu, *J. Optoelectron. Adv. Mater.* **3**, 861 (2001)
- G. Hema Chandra, J.P. de la Cruz, *J. Cryst. Growth* **354**, 67 (2012)
- G. Suresh Babu, Y.B.K. Kumar, P.U. Bhaskar, V.S. Raja, *Semicond. Sci. Technol.* **23**, 85023 (2008)
- J. Xu, Q. Yang, W. Kang, X. Huang, C. Wu, L. Wang, L. Luo, W. Zhang, C.S. Lee, *Part. Part. Syst. Charact.* **32**, 840 (2015)
- D.M. Bishop, B.E. Mccandless, H. Richard, D.B. Mitzi, R.W. Birkmire, *IEEE J. Photovolt.* **5**, 390 (2015)